

# Inducing Axial Chirality in a “Geländer” Oligomer by Length Mismatch of the Oligomer Strands\*\*

Michel Rickhaus, Linda Maria Bannwart, Markus Neuburger, Heiko Gsellinger, Kaspar Zimmermann, Daniel Häussinger, and Marcel Mayor\*

Dedicated to Professor Fritz Vögtle on the occasion of his 75th birthday

**Abstract:** Helical molecules are not only esthetically appealing due to their structural beauty, they also display unique physical properties as a result of their chirality. We describe herein a new approach to “Geländer” oligomers by interlinking two oligomer strands of different length. To compensate for the dimensional mismatch, the longer oligo(benzyl ether) oligomer wraps around the oligophenyl backbone. The new “Geländer” oligomer **1** was assembled in a sequence of functional-group transformations and cross-coupling steps followed by final cyclizations based on nucleophilic substitution reactions, and was fully characterized, including X-ray diffraction analysis. The isolation of pure enantiomers enabled the racemization process to be studied by circular dichroism spectroscopy.

At the end of the 1990s, Vögtle and co-workers described an entirely new class of chiral polyaromatic compounds.<sup>[1]</sup> In contrast to the well-established helicenes<sup>[2]</sup> (Figure 1 b), which resemble the steps of a helical staircase (Figure 1 a, yellow), these “Geländer”-type oligomers<sup>[3]</sup> (Figure 1 c) combine a *p*-phenylene backbone, as the principal axis, with (hetero)alkyl chains that bridge the phenyl rings. The resulting twist between adjacent phenyl rings gives a chiral structure that resembles the helical bannister of a staircase (Figure 1 a, blue).

Despite the different conceptual approach, Vögtle’s “Geländer”-type oligomers showed chiroptical properties comparable to helicenes, namely, intense Cotton effects and high degrees of optical rotation. In contrast to helicenes, the “Geländer”-type oligomers show a high tendency to racemize. Vögtle and co-workers improved the enantiomeric stability by incorporating bulky substituents (R in Figure 1 e) into the oligomeric backbone, which raised the racemization

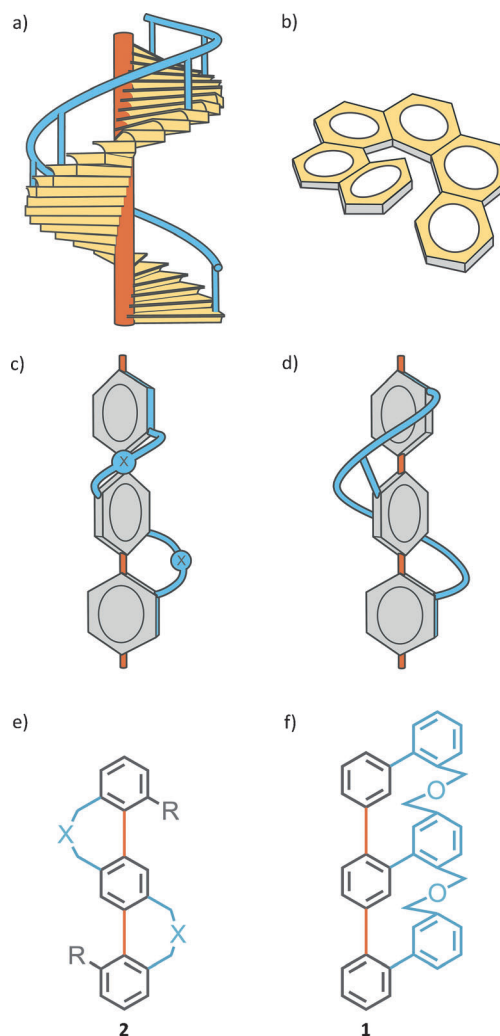


**Figure 1.** Schematic representations of different types of helical structures (only one enantiomer is shown). a) Helical staircase with a central propagation axis (orange), steps (yellow), and a bannister (blue). b) [6]Helicene. c) “Geländer” oligomer described by Vögtle and co-workers, in which two bridges interlink the central *p*-phenylene unit with the two end phenyl groups. d) Schematic representation and f) structural formula of the new “Geländer” oligomer **1** described, in which a second elongated oligomer (blue) ensnares all three rings. e) Structural formula of the “Geländer” oligomer in (c), with X = S or C(CO<sub>2</sub>Me)<sub>2</sub>; R = H or Me.

[\*] M. Rickhaus, L. M. Bannwart, Dr. M. Neuburger, H. Gsellinger, K. Zimmermann, Dr. D. Häussinger, Prof. Dr. M. Mayor  
Department of Chemistry, University of Basel  
St. Johannis-Ring 19, 4056 Basel (Switzerland)  
E-mail: marcel.mayor@unibas.ch

Prof. Dr. M. Mayor  
Institute for Nanotechnology (INT)  
Karlsruhe Institute of Technology (KIT)  
P. O. Box 3640, 76021 Karlsruhe (Germany)

[\*\*] We acknowledge Prof. Dr. Willem Klopper for fruitful discussions and financial support by the Swiss National Science Foundation (SNF).

Supporting information for this article is available on the WWW under <http://dx.doi.org/10.1002/anie.201408424>.

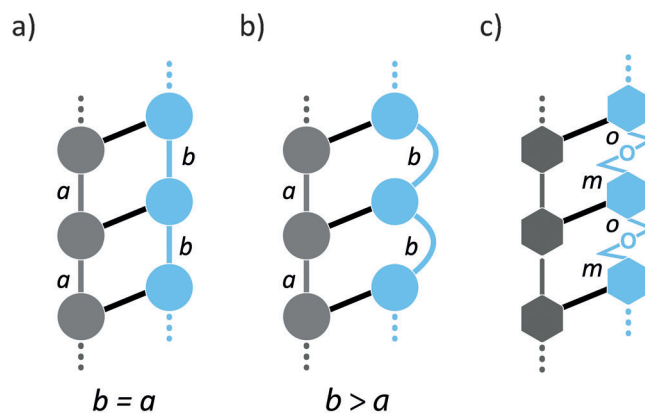
barrier  $\Delta G^\ddagger$  above 22 kcal mol<sup>-1</sup>. Inspired by these results, Rathore and co-workers<sup>[4]</sup> mounted bulky substituents onto the bridging structures. Their synthetic strategy even allowed quadruply bridged pentaphenylenes to be accessed. The racemization barriers in these systems, however, were significantly lower ( $\Delta G^\ddagger \approx 12$  kcal mol<sup>-1</sup>). Although racemization processes in bridged biphenyl systems have been studied extensively,<sup>[5]</sup> investigations on higher oligomeric systems are rare. Enantiomerically pure samples of “Geländer” oligomers not only racemize quickly, but they are even more likely to adopt an achiral *meso* conformation. To display a *meso* form, the structure needs an internal element of symmetry (a point of inversion in the case of “Geländer” oligomers). The synthetic strategies used to access all “Geländer” oligomers result in structures with high degrees of symmetry, which allow the adoption of *meso* forms. Even more importantly, the conformation of one bridge does not necessarily relate to the other—the “helical information” is not relayed across the structure. It ultimately allows each bridge to independently adopt either an *M* or a *P* conformation. The actual chirality of the molecule becomes, in principle, a statistical process, with the *meso* form (*M,P*)/(*P,M*) being twice as likely to occur than either the (*M,M*) or (*P,P*) enantiomers. To the best of our knowledge, all the solid-state structures reported so far include the achiral *meso* form, even when the single crystals were grown from optically pure samples.

We present here a new approach to “Geländer”-type structures to overcome the formation of the *meso* form. The design concept is displayed in Figure 2. If two parallel oligomer chains are interlinked with rigid linkers such as C–C single bonds, a ladder-type structure is obtained if both oligomers have a similar spacing between neighboring connection points (Figure 2a,  $b = a$ ). However, if the periodicity of one oligomer is increased with respect to the other ( $b > a$ ), the two oligomeric chains must compensate for the length mismatch. If rigid subunits are involved, the only way to overcome this discrepancy in length is to wrap the longer oligomer around the shorter one (Figure 2b,c), while the subunits relay the chirality and ensure a continuous helicity. Such a concept tackles both reasons for the formation of the *meso* structure simultaneously: The system can no longer adopt a conformation with a point of inversion, and the helicity is now communicated across the entire structure.

Here we report the first successfully synthesized and fully characterized “Geländer”-type oligomer **1** with a terphenyl backbone and a bannister oligomer consisting of phenyl subunits bridged by *para*-benzyl ether groups (Figures 1 f and 2c). The stiffness and the structural integrity of the *para*-xylene subunit of the longer oligomer allow exclusive formation of the two axially chiral enantiomers as the ground-state conformers. The structure still displays the spirit of Vögtle’s design with a terphenyl backbone, but instead of solely interlinking both biphenyl subunits with independent bridging structures, the entire oligo(*para*-benzyl ether) structure is wrapped around the terphenyl backbone. The result is a structure that resembles a dance ribbon pirouetting around its handling stick.

The synthesis of the “Geländer” oligomer **1** started from commercially available 2-bromo-5-nitroaniline (**3**; Scheme 1).

Side View:



Top View:

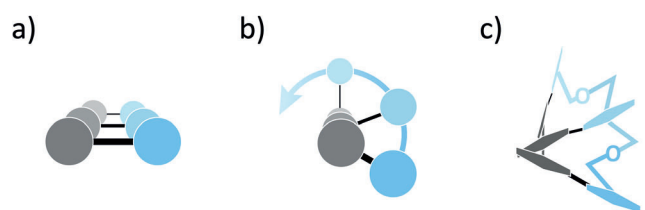
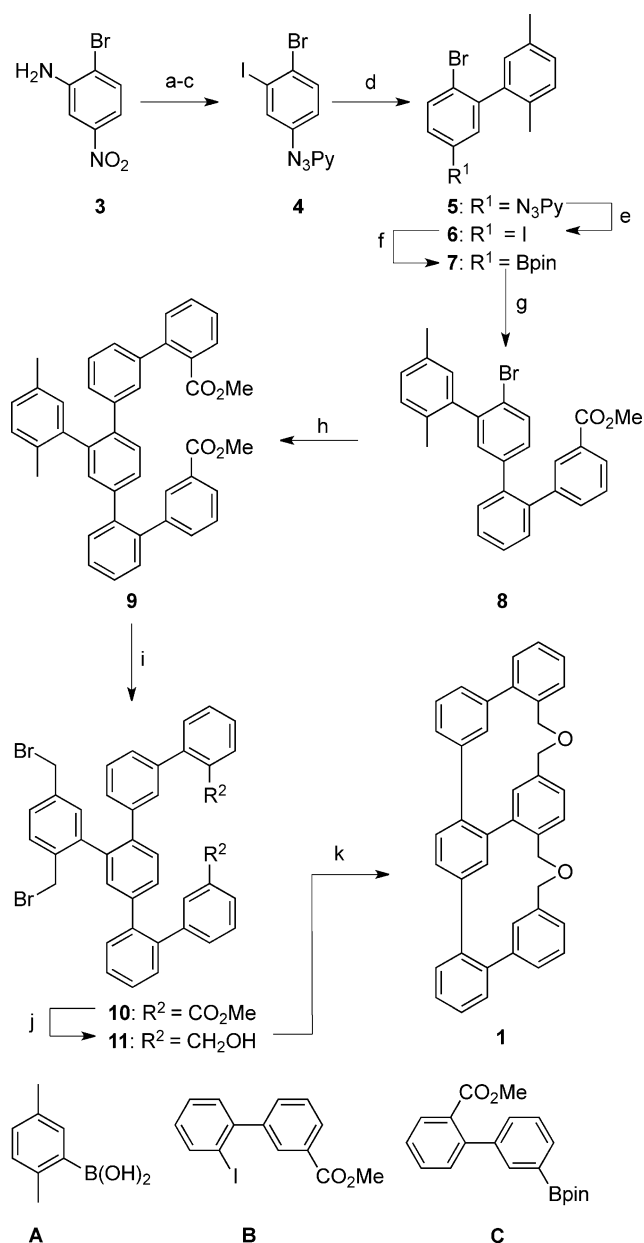


**Figure 2.** General concept of the new type of “Geländer” oligomer. a) If  $a = b$ , the resulting structure resembles a ladder. b) If  $b > a$ , the structure adopts a helical conformation. c) The structure of the new “Geländer” oligomer was designed such that the two adjacent non-backbone phenyl rings (blue) are interlinked in a “*meta* to *ortho*” fashion.

The amino group is converted into an iodine substituent via the corresponding diazonium salt. Subsequently, the nitro group is reduced and converted into a triazene, which acts as a masked leaving group. The obtained building block **4** with three different functional groups in positions 1, 3, and 4 is ideally suited as the central synthon for the stepwise attachment of all the required aromatic rings. Under Suzuki–Miyaura cross-coupling conditions, the boronic acid **A** substitutes the iodine to provide intermediate **5**. Treatment of **5** with MeI transforms the triazene into the iodine **6**, which is subsequently converted into the pinacol borane **7** by applying Hosomi–Miyaura borylation conditions. To cross-couple biphenyls **6** and **B** it was necessary to convert **6** into the borane **7**, since all attempts to borylate **B** provided a mixture of regioisomers. The borylated fragment **7** allowed two consecutive Suzuki–Miyaura cross-coupling reactions with **B** and **C** to be carried out to afford intermediates **8** and **9**. Both cross-coupling steps required catalysts optimized for sterically demanding systems.<sup>[6]</sup> Intermediate **9** provides the entire required carbon atom skeleton for the target structure **1**, and was isolated in 19% overall yield over 8 steps (longest linear sequence). Benzylic bromination afforded **10** in excellent yield. Subsequent reduction of the ester groups provided **11** quantitatively, which is decorated with the functional groups required for intramolecular bridging by nucleophilic substitution. To our surprise, this final cyclization step turned out to



**Scheme 1.** Synthesis of target compound **1**. Reaction conditions: a) 1.  $\text{BF}_3 \cdot \text{OEt}_2$ ,  $\text{ONO}t\text{Bu}$ , THF,  $-30^\circ\text{C}$  to RT, 3 h; 2.  $\text{I}_2$ , KI, MeCN, RT, 30 min, 85–97%; b) Fe, HCl, EtOH,  $0^\circ\text{C}$ , 2 h, 94%; c) 1.  $\text{BF}_3 \cdot \text{OEt}_2$ ,  $\text{ONO}t\text{Bu}$ ,  $\text{CH}_2\text{Cl}_2$ ,  $-30^\circ\text{C}$  to  $-5^\circ\text{C}$ , 15 min; 2. pyrrolidine,  $\text{K}_2\text{CO}_3$ , RT, 15 min, 95%; d) **A**,  $[\text{Pd}(\text{PPh}_3)_2\text{Cl}_2]$ ,  $\text{K}_2\text{CO}_3$ , THF/ $\text{H}_2\text{O}$  4:1,  $60^\circ\text{C}$ , overnight, 88–99%; e) MeI,  $120^\circ\text{C}$ , overnight, 96%; f)  $[\text{Pd}(\text{dppf})\text{Cl}_2]$ , KOAc,  $\text{B}_2\text{pin}_2$ , dioxane,  $100^\circ\text{C}$ , overnight, 53%; g) **B**, XPhos Pd G2,  $\text{K}_2\text{CO}_3$ , toluene,  $110^\circ\text{C}$ , 1–2 days, 58–84%; h) **C**, SPhos Pd G2,  $\text{K}_2\text{CO}_3$ , toluene/ $\text{H}_2\text{O}$ ,  $110^\circ\text{C}$ , 1–3 days, 50%; i) NBS, DBP,  $\text{CCl}_4$ ,  $75^\circ\text{C}$ , 1 h, 87% to > 99%; j) DIBAL-H,  $\text{CH}_2\text{Cl}_2$ , RT, 30 min, > 99%; k) 1. NaH, THF, reflux, 12 h, 30% for the monocyclized intermediate; 2. NaH,  $[\text{D}_8]\text{THF}$ , reflux, 2–3 days, 28%. Bpin = 4,4,5,5-tetramethyl-1,3,2-dioxaborolane, DBP = dibenzoylperoxide, NBS = *N*-bromosuccinimide,  $\text{N}_3\text{Py}$  = diazenylpyrrolidine.

be very challenging, probably because of both the limited stability of the bridging benzylic ether subunits and competing intermolecular reactions. Ultimately, the most efficient method to obtain **1** was to subject **11** to basic reaction

conditions and to stop the reaction at the point when the highest quantity of the monocyclized product was observed in the reaction mixture. Interestingly, only one of the four theoretically possible monocyclized isomers was observed. After this point, the concentration of the monocyclized product decreased, but the desired doubly cyclized compound **1** could only be detected in trace amounts. Consequently, the monocyclized product was isolated and purified before being subjected again to basic conditions to undergo the second cyclization step. This step was performed in  $[\text{D}_8]\text{THF}$  at  $60^\circ\text{C}$  directly in an NMR tube, and the exclusive formation of the target compound **1** was monitored by  $^1\text{H}$  NMR spectroscopy.

Purification of **1** by flash column chromatography (on acidic and passivated silica and Alox) resulted in substantial decomposition of the product. Therefore, crude **1** was subjected directly to HPLC on a chiral stationary phase (Chiralpak IA, eluent *n*-hexane/2-propanol 99:1,  $1\text{ mL min}^{-1}$ ,  $T = 25^\circ\text{C}$ ) to separate the two enantiomers of **1** and afford each enantiomer in about 14% yield (> 99% *ee*). Once isolated, each enantiomer showed prolonged stability towards air and moisture as well as solubility in most organic solvents. Compound **1** was fully characterized by  $^1\text{H}$  and  $^{13}\text{C}$  NMR spectroscopy, UV/Vis spectroscopy, high-resolution mass spectrometry (HR-ESI), and single-crystal X-ray diffraction (see the Supporting Information). The  $^1\text{H}$  NMR spectrum showed distinct doublets for each of the diastereotopic hydrogen atoms of the bridge, which indicates a slow racemization process on the NMR timescale. Each enantiomer showed only one set of signals and their spectra were identical, thus indicating that the two fractions obtained by HPLC on the chiral stationary phase were indeed enantiomers. Laborious 2D NMR spectroscopy allowed all the observed signals in the  $^1\text{H}$  and  $^{13}\text{C}$  NMR spectra to be fully assigned. As a result of the high steric constraints and the resulting relaxation times, a suitable  $^{13}\text{C}$  NMR spectrum of **1** could be obtained indirectly. The  $^{13}\text{C}$  NMR, UV/Vis, and HRMS spectra for both enantiomers were also identical. Further evidence that the isolated fractions were enantiomers was provided by circular dichroism (CD) measurements (Figure 4a). Cotton effects were observed at 240, 220, and 200 nm, with opposite signs for the two enantiomers.

On the basis of the design of the “Geländer” oligomer **1**, we anticipated its conformation to be stiff and thus its helicity to be stable at room temperature. To properly identify the helicity of both enantiomers, we grew single crystals suitable for X-ray analysis from a freshly separated, diluted solution of one of the enantiomers in diethyl ether by slow evaporation within seven days. The solid-state structure provided a surprise: the crystallized sample was the racemate of **1** with two molecules of each enantiomer in the unit cell. Different views of the solid-state structure of **1** are displayed in Figure 3. The solid-state structure corroborates the helical wrapping of the benzyl ether oligomer (blue carbon atoms in Figure 3a and b) in a banister-like manner around the oligophenyl backbone (gray carbon atoms in Figure 3a and b), as postulated in the molecular design. The torsion angles between the two adjacent backbone aromatic rings were found to be  $81.5^\circ$  and  $64.3^\circ$ , which corresponds to a total twist along the entire oligophenylene backbone of  $147.3^\circ$ .

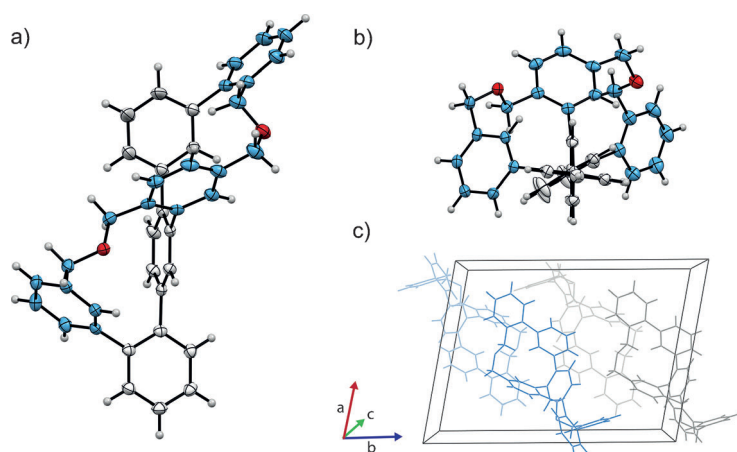


**Figure 3.** The X-ray structure of racemic **1** from different view points (rotation ellipsoids at 50% probability). a) Side view and b) front view of one enantiomer. c) The unit cell, which contains two molecules of each enantiomer. Color code: bridge: blue, backbone: gray, H: white, O: red (a, b); enantiomers: blue, gray (c).

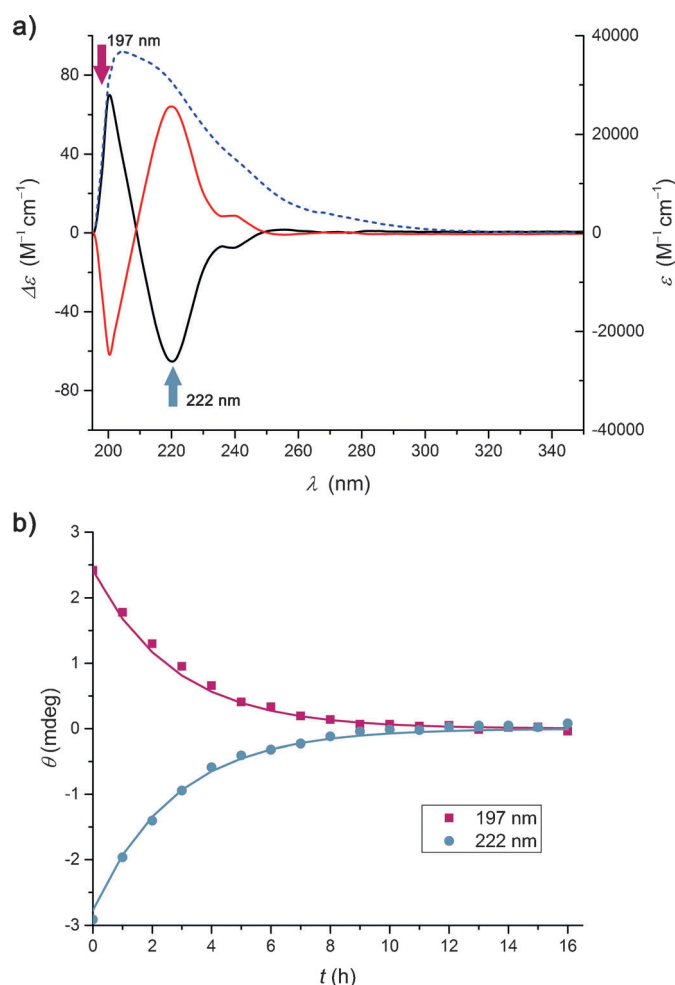


**Figure 4.** a) UV/Vis spectra (dashed blue line) of racemic **1** and CD traces for the separated enantiomers (black and red lines). The spectra were recorded in *n*-hexanes/2-PrOH (99:1) at 25 °C. Absorption maxima and distinct Cotton effects were observed at 240, 220, and 200 nm. The arrows indicate the wavelengths used to observe the decay of the CD signal over time. b) The decay of the CD signal over time was observed at 222 and 197 nm at 25 °C. The racemic state was reached in approximately 10 h.

As the formation of racemic crystals came as a surprise, we were curious about the racemization process. To investigate the racemization kinetics of **1**, the disappearance of the two most intense CD signals (197 and 222 nm) of a freshly purified enantiomer were recorded as a function of time at 25 °C (Figure 4b). Racemization was almost complete within 10 h. A plot of time (*t*) against ln(*A*) (see the Supporting Information) allowed the rate of racemization to be determined as  $k_{\text{rac}} = 5.040 \times 10^{-6} \text{ s}^{-1}$  ( $k_{\text{rac}}^{222 \text{ nm}} = 5.146 \pm 0.05 \times 10^{-6} \text{ s}^{-1}$ ,  $k_{\text{rac}}^{197 \text{ nm}} = 4.936 \pm 0.05 \times 10^{-6} \text{ s}^{-1}$ ), which results in half-lives of 3.82 h ( $t_{1/2}^{222 \text{ nm}} = 3.74 \text{ h}$ ,  $t_{1/2}^{197 \text{ nm}} = 3.90 \text{ h}$ ) at 25 °C. The data further allowed the energy barrier for racemization to be determined (see the Supporting Information) as  $\Delta G^\ddagger = 97.55 \pm 0.1 \text{ kJ mol}^{-1}$  (23.3 kcal mol<sup>-1</sup>) at 25 °C. This value is in a similar range as those reported for the most stable “Geländer” oligomers by Vögtle and co-workers. As postulated during the design of the “Geländer” oligomer, the racemization process does

not involve a chiroptically silent, thermodynamically favored intermediate (in other words, no *meso* form). Racemization most likely occurs by rotation around the single bond in the central biphenyl subunit, along with an unwrapping and rewrapping of the benzyl ether oligomer and inversion of helicity.

In summary, a new type of a “Geländer”-type terphenyl oligomer was synthesized, fully characterized, and its racemization behavior studied. Compared to the previously known “Geländer”-type oligomers, the new system interlinks all three terphenyl rings through an oligo(benzyl ether) as a single bridge (instead of two) and thus lacks a point of inversion. As a result, the structure exists exclusively in the form of two stereoisomers, a pair of enantiomers. This structural characteristic leads to a uniform racemization pathway without an achiral intermediate *meso* structure. The high racemization barrier allowed the separation of both enantiomers by HPLC on a chiral stationary phase. These enantiomers subsequently underwent racemization. X-ray diffraction analysis of the racemic single crystals confirmed the helical structure of the “Geländer”-type oligomer.

Received: August 21, 2014

Published online: November 3, 2014

**Keywords:** atropisomerism · Geländer oligomers · helical structures · hexaphenyls · racemization

- [1] B. Kiupel, C. Niedert, M. Nieger, S. Grimme, F. Vögtle, *Angew. Chem. Int. Ed.* **1998**, *37*, 3031–3034; *Angew. Chem.* **1998**, *110*, 3206–3209.
- [2] For an excellent review, see M. Gingras, *Chem. Soc. Rev.* **2013**, *42*, 968–1006, and references therein.
- [3] “Geländer” is the German word for banister.
- [4] M. Modjewski, S. V. Lindeman, R. Rathore, *Org. Lett.* **2009**, *11*, 4656–4659.
- [5] Representative examples: a) K. Ohkata, R. L. Paquette, L. A. Paquette, *J. Am. Chem. Soc.* **1979**, *101*, 6687–6693; b) K. Müllen, W. Heinz, F. Klärner, W. R. Roth, I. Kindermann, O. Adamczak,

- M. Wette, J. Lex, *Chem. Ber.* **1990**, *123*, 2349–2371; c) J. Rotzler, H. Gsellinger, M. Neuburger, D. Vonlanthen, D. Häussinger, M. Mayor, *Org. Biomol. Chem.* **2011**, *9*, 86; d) J. Rotzler, H. Gsellinger, A. Bihlmeier, M. Gantenbein, D. Vonlanthen, D. Häussinger, W. Klopper, M. Mayor, *Org. Biomol. Chem.* **2012**, *10*, 110–118; e) J. Rotzler, H. Gsellinger, A. Bihlmeier, M. Gantenbein, D. Vonlanthen, D. Häussinger, W. Klopper, M. Mayor, *Org. Biomol. Chem.* **2013**, *11*, 110; f) K. Takaishi, M. Kawamoto, K. Tsubaki, *Org. Lett.* **2010**, *12*, 1832–1835.
- [6] S. L. Buchwald, N. C. Bruno, *The Strem Chemiker Vol. XXVII* **2014**, 1.
-